

Electrical Conductivity and Rheology of Carbon-Filled Liquid Crystal Polymer Composites

Julia A. King, Faith A. Morrison, Jason M. Keith, Michael G. Miller, Ryan C. Smith, Mariana Cruz, Amanda M. Neuhalfen, Rodwick L. Barton

Department of Chemical Engineering, Michigan Technological University, Houghton, Michigan 49931-1295

Received 21 October 2005; accepted 12 December 2005

DOI 10.1002/app.23914

Published online in Wiley InterScience (www.interscience.wiley.com).

ABSTRACT: One emerging market for electrically conductive resins is for bipolar plates for use in fuel cells. Adding carbon fillers to thermoplastic resins increases composite electrical conductivity and viscosity. Current technology often adds as much of a single type of carbon filler as possible to achieve the desired conductivity, while still allowing the carbon-filled thermoplastic matrix material to be extruded and molded into a bipolar plate. In this study, varying amounts of two different types of carbon, one carbon black and one synthetic graphite, were added to Vectra A950RX liquid crystal polymer. The resulting single filler composites were then tested for electrical conductivity and rheological properties. The electrical conductivity followed that typically seen in polymer composites with a percolation

threshold at 4 vol % for carbon black and at 15 vol % for synthetic graphite. Over the range of shear rates studied, the viscosity followed a shear-thinning power law model with power-law exponent $(n - 1) = -0.5$ for neat Vectra A950RX and $(n - 1) = -0.7$ for highly filled composite materials. Viscosity increased with increasing filler volume fraction for all shear rates. The viscosity-enhancement effect was more rapid for the composites containing carbon black when compared with those containing synthetic graphite. © 2006 Wiley Periodicals, Inc. *J Appl Polym Sci* 101: 2680–2688, 2006

Key words: composites; fillers; rheology; liquid crystalline polymers; extrusion

INTRODUCTION

Most polymer resins are electrically insulating. Increasing the electrical conductivity of these resins allows them to be used in other applications. One emerging market for electrically conductive resins is for bipolar plates for use in fuel cells. The bipolar plate separates one cell from the next, with this plate carrying hydrogen gas on one side and air (oxygen) on the other side. Bipolar plates require high thermal and electrical conductivity (to conduct heat and to minimize ohmic losses), low gas permeability, and good dimensional stability.

Electrical resistivity (1/electrical conductivity) values in ohm-cm for various materials are typically 10^{14} – 10^{17} for polymers, 10^{-2} for carbon black, 10^{-5} for high purity synthetic graphite, and 10^{-6} for metals such as aluminum and copper. One approach to improving the electrical conductivity of a polymer is through the

addition of a conductive filler material, such as carbon and metal.^{1–14} Currently, a single type of graphite powder is typically used in thermosetting resins (often a vinyl ester) to produce a thermally and electrically conductive bipolar plate material.^{15–18} Thermosetting resins cannot be remelted.

In this work, researchers performed compounding runs followed by injection molding of carbon-filled Vectra A950RX. Vectra is a thermoplastic that can be remelted and used again. One carbon black and one synthetic graphite were studied. Material's characterization tests included volumetric electrical resistivity and capillary rheometry to determine the viscosity parameters. The goal of this project was to determine how various amounts of these single carbon fillers affected the composite electrical resistivity (1/electrical conductivity) and viscosity. These results may improve manufacturing procedures for fuel cell bipolar plates.

MATERIALS AND EXPERIMENTAL METHODS

Materials

The matrix used for this project was Ticona's Vectra A950RX liquid crystal polymer (LCP), which is a highly ordered thermoplastic copolymer consisting of 73 mol % hydroxybenzoic acid and 27 mol % hydroxynaphtholic acid. This LCP has the properties

Correspondence to: J. A. King (jaking@mtu.edu).

Contract grant sponsor: Department of Energy; contract grant number: DE-FG02-04ER63821.

Contract grant sponsor: National Science Foundation; contract grant numbers: DGE-0333401, DMI-0456537.

Contract grant sponsor: U.S. Department of Education; contract grant number: P200A030192.

TABLE I
Properties of Ticona's Vectra A950RX¹⁹

Melting point	280°C
Tensile modulus (1 mm/min)	10.6 GPa
Tensile stress at break (5 mm/min)	182 MPa
Tensile strain at break (5 mm/min)	3.4%
Flexural modulus at 23°C	9.1 GPa
Notched Izod impact strength at 23°C	95 KJ/m ²
Density at 23°C	1.40 g/cc
Volumetric electrical resistivity at 23°C	10 ¹⁵ ohm-cm
Surface electrical resistivity	10 ¹⁴ ohm
Thermal conductivity at 23°C	0.2 W/mK (approx.)
Humidity absorption (23°C/50% RH)	0.03 wt %
Mold shrinkage-parallel	0.0%
Mold shrinkage-normal	0.7%
Coefficient of linear thermal expansion (parallel)	0.04 × 10 ⁻⁴ /°C
Coefficient of linear thermal expansion (normal)	0.38 × 10 ⁻⁴ /°C

needed for bipolar plates, namely high dimensional stability up to a temperature of 250°C, extremely short molding times (often 5–10 s), exceptional dimensional reproducibility, chemically resistant in acidic environments present in a fuel cell, and a low hydrogen gas permeation rate.^{19,20} The properties of this polymer are shown in Table I.¹⁹

The first filler used in this study was Ketjenblack EC-600 JD. This is an electrically conductive carbon black available from Akzo Nobel. The highly branched, high surface area carbon black structure allows it to contact a large amount of polymer, which results in improved electrical conductivity at low carbon black concentrations (often 5–7 wt %). The properties of Ketjenblack EC-600 JD are given in Table II.²¹ The carbon black is in the form of pellets that are 100 μm to 2 mm in size and, upon mixing into a polymer, easily separate into primary aggregates 30–100 nm long.²¹ Figure 1 shows a diagram of this carbon black structure.²¹

Table III shows the properties of Asbury Carbons' Thermocarb TC-300, which is a primary synthetic graphite that was previously sold by Conoco.^{22,23} Thermocarb TC-300 is produced from a thermally treated highly aromatic petroleum feedstock and con-

TABLE II
Properties of Akzo Nobel Ketjenblack EC-600 JD²¹

Electrical resistivity	0.01–0.1 ohm-cm
Aggregate size	30–100 nm
Specific gravity	1.8 g/cm ³
Apparent bulk density	100–120 kg/m ³
Ash content (max)	0.1 wt %
Moisture (max)	0.5 wt %
BET surface area	1250 m ² /g
Pore volume	480–510 cm ³ /100g

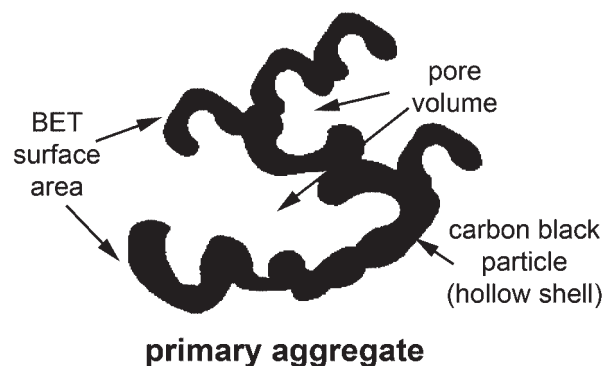


Figure 1 Structure of Ketjenblack EC-600 JD.²¹

tains very few impurities. Figure 2 shows a photomicrograph of this synthetic graphite.²²

Electrical resistivity and viscosity were measured on composites containing varying amounts of these carbon fillers in Vectra A950RX. The concentrations (shown in wt % and the corresponding vol %) for these single filler composites are shown in Tables IV and V. Note that additional parameters that will be defined later in this article also appear in these tables. Prior work in nylon 6,6 and polycarbonate has shown that the concentrations selected for these fillers will yield electrically conductive resins.^{24,25} For bipolar plate applications, typically 60–70 wt % synthetic graphite is used.¹⁵

TABLE III
Properties of Thermocarb TC-300 Synthetic Graphite^{22,23}

Filler property	Thermocarb TC-300 synthetic graphite
Carbon content (wt %)	99.91
Ash (wt %)	<0.1
Sulfur, wt%	0.004
Density (g/cc)	2.24
BET surface area (m ² /g)	1.4
Thermal conductivity at 23°C (W/mK)	600 in "a" crystallographic direction
Electrical resistivity of bulk carbon powder at 150 psi, 23°C, parallel to pressing axis (ohm-cm)	0.020
Particle shape	Acicular
Particle aspect ratio	1.7
Sieve analysis (wt %)	
+600 μm	0.19
+500 μm	0.36
+300 μm	5.24
+212 μm	12.04
+180 μm	8.25
+150 μm	12.44
+75 μm	34.89
+44 μm	16.17
–44 μm	10.42

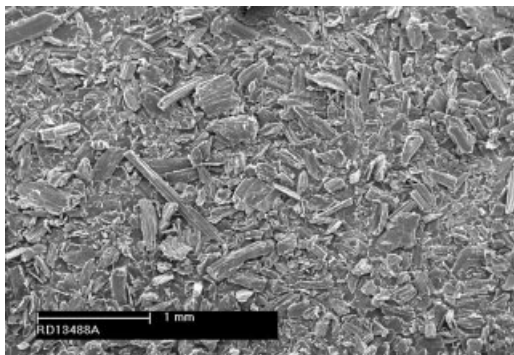


Figure 2 Photomicrograph of Thermocarb TC-300 synthetic graphite.²²

Test specimen fabrication

For this entire project, the fillers were used as received. Vectra A950RX was dried in an indirect heated dehumidifying drying oven at 150°C and then stored in moisture barrier bags.

The extruder used was an American Leistritz Extruder Corp. Model ZSE 27. This extruder has a 27 mm corotating intermeshing twin screw with 10 zones and a length/diameter ratio of 40. Figure 3 shows the screw design. It was chosen to allow a large concentration of filler to mix with the matrix material and thereby achieve the maximum possible conductivity. The Vectra polymer pellets were introduced in Zone 1. A side stuffer located at Zone 5 was used to introduce the carbon fillers into the polymer melt. Two Schenck AccuRate gravimetric feeders were used to accurately control the amount of each material added to the extruder.

After passing through the extruder, the polymer strands (3 mm in diameter) entered a water bath and then a pelletizer that produced nominally 3 mm long pellets. After compounding, the pelletized composite resin was dried again and then stored in moisture barrier bags prior to injection molding.

A Niigata injection molding machine, model NE85UA₄, was used to produce test specimens. This

TABLE IV
Single Filler Loading Levels of Ketjenblack EC-600 JD in Vectra A950RX and Power Law Viscosity Correlation Parameters

Filler wt %	Filler vol %	m (Pa·s ^{<i>n</i>})	n (dimensionless)
0.0	0.0	690	0.54
2.5	1.9	1,300	0.53
4.0	3.1	2,700	0.49
5.0	3.9	4,700	0.45
6.0	4.7	7,500	0.41
7.5	6.0	18,000	0.35
10.0	8.0	50,000	0.29
15.0	12.1	N/A	N/A

TABLE V
Single Filler Loading Levels of Thermocarb TC-300 in Vectra A950RX and Power Law Viscosity Correlation Parameters

Filler wt %	Filler vol %	m (Pa·s ^{<i>n</i>})	n (dimensionless)
0.0	0.0	690	0.54
10.0	6.5	611	0.58
15.0	9.9	N/A	N/A
20.0	13.5	700	0.58
25.0	17.2	N/A	N/A
30.0	21.1	890	0.58
40.0	29.3	2,300	0.51
50.0	38.5	6,200	0.45
55.0	43.3	N/A	N/A
60.0	48.4	22,000	0.36
65.0	53.7	N/A	N/A
70.0	59.3	80,000	0.29
75.0	65.2	N/A	N/A

machine has a 40 mm diameter single screw with a length/diameter ratio of 18. The lengths of the feed, compression, and metering sections of the single screw are 396, 180, and 144 mm, respectively.

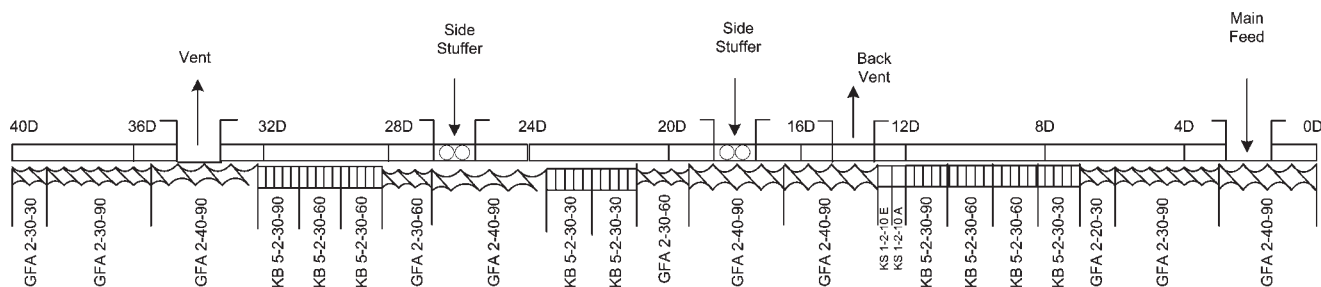
The temperature profile typically used was 280°C in Zone 1 (nearest feed hopper), 307°C in Zones 2 and 3, and 315°C in Zone 4. A four cavity mold was used to produce 3.2-mm thick ASTM Type I tensile bars (end gated) and 6.4 cm diameter disks (end gated). The electrical resistivity and steady shear viscosity of all formulations were determined. Prior to conducting the electrical resistivity tests, the samples were conditioned at 23°C and 50% RH for 88 h and then tested.²⁶

Through-plane electrical resistivity test method

For samples with an electrical resistivity $>10^4$ ohm-cm, through-plane (also called transverse), volumetric electrical resistivity test was conducted. In this method, a constant voltage (typically 100 V) was applied to the as molded test specimen, and the resistivity was measured according to ASTM D257 using a Keithley 6517A Electrometer/High Resistance Meter and an 8009 Resistivity Test Fixture.²⁷ The Keithley 6524 High Resistance Measurement Software was used to automate the resistivity measurement. For each formulation, a minimum of six specimens were tested. Each test specimen was an injection-molded disk that was 6.4 cm in diameter and 3.2 mm thick.

In-plane electrical resistivity test method

The volumetric in-plane (also called longitudinal) electrical resistivity was measured on all samples with an electrical resistivity $<10^4$ ohm-cm. Test specimens cut from the center gauge portion of a tensile bar were surface ground on all sides and then cut into sticks 2 mm wide by 2 mm thick by 25.4 mm long. Typically



For Screw Type Elements

GFA-d-ee-ff
 G = co-rotating
 F = conveying
 A = Free-Meshing
 d = number of threads
 ee = pitch (length in millimeters for one complete rotation)
 ff = length of screw elements in millimeters

Kneading Blocks

KBj-d-kk-l
 KB = kneading block
 j = number of kneading segments
 d = number of threads
 k = length of kneading blocks in millimeters
 l = twisting angle (°) of the individual kneading segments

Kneading Disks

KS1-d-hh-i
 KS1 = Kneading disk
 d = number of threads
 h = length of kneading disk in millimeters
 i = A for initial disk and E for end disk

Zones

0D to 4D is Zone 1
 4D to 8D is Zone 2 and Heating Zone 1
 8D to 12D is Zone 3 and Heating Zone 2
 12D to 16D is Zone 4 and Heating Zone 3
 16D to 20D is Zone 5 and Heating Zone 4
 20D to 24D is Zone 6 and Heating Zone 5
 24D to 28D is Zone 7 and Heating Zone 6
 28D to 32D is Zone 8 and Heating Zone 7
 32D to 36D is Zone 9 and Heating Zone 8
 36D to 40D is Zone 10 and Heating Zone 9
 Nozzle is Heating Zone

Figure 3 Extruder screw design.

for each formulation, a total of six specimens were cut from a single tensile bar, and three tensile bars were typically used to obtain a total of eighteen test specimens.²⁸ These samples were then tested using the four-probe technique. This technique measures resistivity by applying a constant current (typically 5–10 mA) and measuring the voltage drop over the center 6 mm of the sample.⁸ A Keithley 224 Programmable Current Source and Keithley 182 Digital Sensitive Voltmeter were used. Equation (1) below is then used to calculate the electrical resistivity.

$$ER = \frac{(\Delta V)(w)(t)}{(i)(L)} \quad (1)$$

where ER is the electrical resistivity (ohm-cm), ΔV is the voltage drop over center 0.6 cm of sample (volts) w is the sample width (cm) t is the sample thickness (cm) i is the current (amps), and L is the length over which ΔV is measured (0.6 cm).

Filler orientation test method

To determine the orientation of the synthetic graphite, a polished composite sample was viewed using an optical microscope. For each formulation, an in-plane electrical resistivity sample was cast in epoxy so that the direction of flow induced during the injection molding process, which was also the direction of ER

measurement (lengthwise direction), would be viewed. For the through-plane thermal resistivity samples, the center portion was cut out of a disk and set in epoxy such that through the sample thickness (3.2 mm) face could be viewed. The samples were then polished and viewed using an Olympus BX60 reflected light microscope at a magnification of 100× or 200×. The images were then processed using Adobe Photoshop 5.0 and the Image Processing Tool Kit version 3.0. For each formulation, the orientation was determined by viewing typically 1000–2000 particles.

Capillary rheometer test method

To determine viscosity, a Goettfert Rheo-Tester 1000, which is a capillary rheometer, was used. For low shear rates, a 200 bar pressure transducer was used, and a 1400 bar pressure transducer was used for high shear rates. The extruded pellets from all formulations were dried (as described previously) prior to testing. Three different round-hole 180° capillaries were used. Each capillary had a diameter of 1 mm. The length of the three capillaries were 20, 30, and 40 mm. For each capillary, the same formulation was tested three times at 300°C, above Vectra’s melting point of 280°C. The viscosities at the following apparent shear rates, $\dot{\gamma}_{ar}$ were determined: 100, 200, 500, 1000, 2000, and 5000 s⁻¹. The apparent shear rate, $\dot{\gamma}_{ar}$ was calculated using eq. (2) shown below:

$$\dot{\gamma}_a = 4Q/\pi R^3 \quad (2)$$

where Q is the volumetric flow rate (in units of mm^3/s) and R is the radius (in units of mm) of the capillary.²⁹ The test method used was ASTM D3835.³⁰ Raw data of pressure drop versus shear rate were corrected for nonparabolic velocity profile by use of the Weissenberg-Rabinowitsch correction. Entrance pressure loss, i.e., the Bagley Correction was measured to be zero in all cases.³¹

RESULTS

Filler orientation results

As discussed previously, the filler orientation angle was measured by optical microscopy. The angle of interest was the deviation of the filler away from the direction of resistivity measurement. All of the angles will be between 0° and 90° . An angle of 0° degrees signifies that the fillers are aligned parallel to the measurement direction. An angle of 90° means that the fillers are perpendicular (transverse) to the measurement direction.

For the in-plane electrical resistivity sample containing 60 wt % Thermocarb TC-300 synthetic graphite in Vectra A950RX, the mean orientation angle was 24° , which indicates that most of the fillers are oriented in the electrical resistivity measurement direction. This photomicrograph is shown elsewhere.³² This result is typical of all the samples in this study, and it agrees with prior work.²⁸

For the through-plane electrical resistivity samples, the mean orientation angle was typically 52° , which indicates that the fillers are primarily oriented transverse to the resistivity measurement direction. This observation agrees with prior work.³³ Figure 4 shows a photomicrograph of a through-plane resistivity sample containing 70 wt % Thermocarb TC-300 synthetic graphite in Vectra A950RX.

Electrical resistivity results

Figure 5 shows the log (electrical resistivity in ohm-cm) for composites containing varying amounts of single fillers as a function of filler volume fraction. In this figure, all the data points have been plotted. Figure 5 follows the typical electrical resistivity curve. At low filler loadings, the electrical resistivity remains similar to that of the pure polymer. Then at a point called the percolation threshold, the resistivity decreases dramatically over a very narrow range of filler concentrations. At higher filler loadings, the electrical resistivity begins to level out again at a value many orders of magnitude lower than that of the pure polymer.^{5,34}

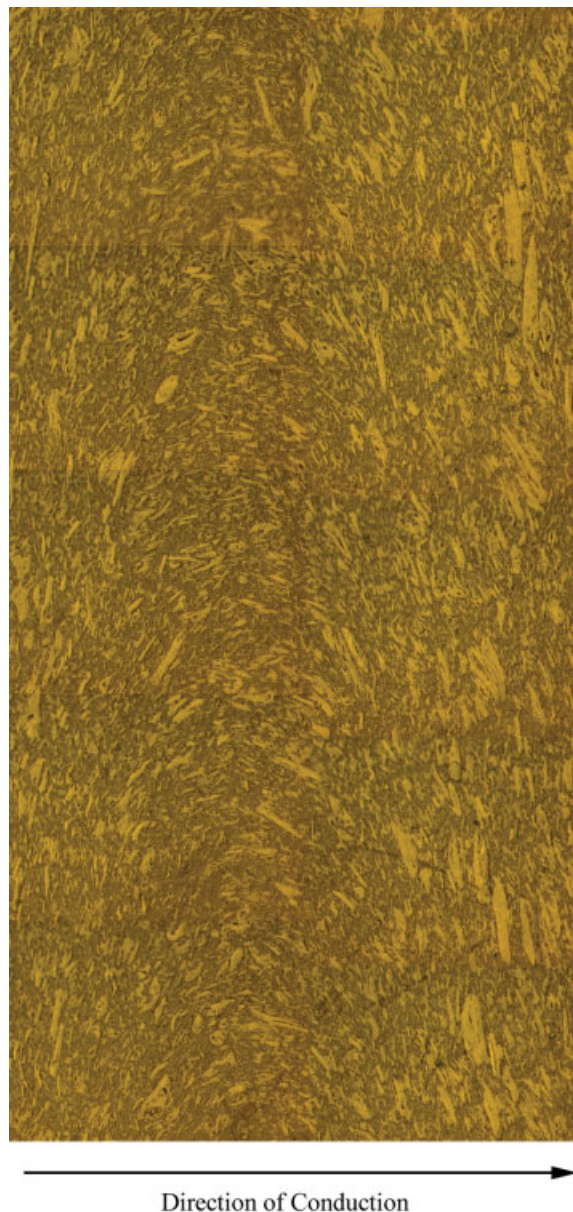


Figure 4 Through-plane electrical resistivity sample containing 70 wt % Thermocarb TC-300 synthetic graphite in Vectra A950RX at $100\times$ magnification. [Color figure can be viewed in the online issue, which is available at www.interscience.wiley.com.]

Figure 5 shows that carbon black is effective at decreasing the electrical resistivity ($1/\text{electrical conductivity}$) at low filler loadings. The pure Vectra A950RX has a mean electrical resistivity of 2.2×10^{16} ohm-cm (vendor literature states 10^{15} ohm-cm).¹⁹ The percolation threshold for carbon black occurs at 4 vol %. At the highest filler concentration, the carbon black produced a mean composite resistivity of 2 ohm-cm (15 wt % = 12.1 vol %). These electrical resistivity results are similar to those reported elsewhere.^{5,21}

Figure 5 shows that the percolation threshold for Thermocarb synthetic graphite occurs at 15 vol %. This

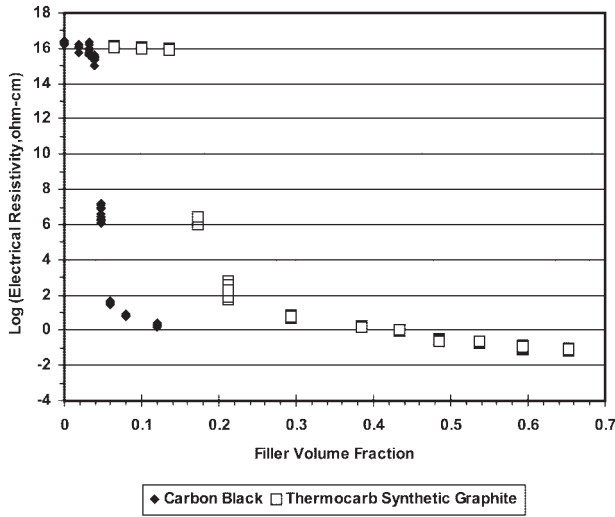


Figure 5 Electrical resistivity results.

higher filler amount needed for the percolation threshold for composites containing Thermocarb is due to the different particle shape/structure and properties of synthetic graphite particles when compared to those for carbon black (see Figs. 1 and 2 and Tables II and III). The composites containing 60 and 70 wt % (48.4 and 59.3 vol %) Thermocarb had mean electrical resistivities of 0.26 and 0.11 ohm-cm, respectively.

Capillary rheometer results

Capillary rheometer tests were conducted on composites containing the amounts of fillers shown below:

1. Thermocarb TC-300: 10, 20, 30, 40, 50, 60, 70 (all in wt %)
2. Ketjenblack EC-600 JD: 2.5, 4, 5, 6, 7.5, 10 (all in wt %)

Composites containing 75 wt % Thermocarb and 15 wt% Ketjenblack were too viscous to test.

Polymer rheological data are typically illustrated in a log–log plot of the viscosity η as a function of the shear rate $\dot{\gamma}$. A horizontal line is indicative of a Newtonian fluid when η is constant. If the viscosity decreases as the shear rate is increased, the fluid is called shear-thinning. LCPs usually exhibit shear thinning behavior.^{35–37} They can also exhibit Newtonian fluid behavior over a narrow range of low shear rates.^{35–37} For Vectra A950RX, vendor data suggests shear-thinning behavior.¹⁹

For capillary fluid flow, the shear stress at the wall τ_R (in units of Pa) is given by

$$\tau_R = \frac{R\Delta P}{2L} \tag{3}$$

where ΔP is the pressure drop (in units of Pa) over the capillary of radius R (in units of mm) and length L (in units of mm). For non-Newtonian fluids, the relationship between the true shear rate at the wall of the capillary $\dot{\gamma}_R$ and the “apparent shear rate” $\dot{\gamma}_a$ (what the shear rate would be for a Newtonian fluid) is given by the following relationship.²⁹

$$\dot{\gamma}_R = \dot{\gamma}_a \left[\frac{1}{4} \left(3 + \frac{d \ln \dot{\gamma}_a}{d \ln \tau_R} \right) \right] \tag{4}$$

Equation (4) is valid for any fluid. The quantity in square brackets is called the Weissenberg-Rabinowitsch correction. For Newtonian fluids, the correction factor is one and $\dot{\gamma}_R = \dot{\gamma}_a$.

For our experiments, the apparent shear rate $\dot{\gamma}_a$ was varied (100, 200, 500, 1000, 2000, and 5000 s⁻¹), and the pressure drop was measured using a pressure transducer. On the basis of eq. (3), the shear stress at the wall τ_R was calculated. A quadratic equation was fit to the τ_R versus $\dot{\gamma}_a$ data, the derivative in eq. (4) was calculated, and the shear rate at the capillary wall $\dot{\gamma}_R$ was determined. Finally, the steady shear viscosity η (in units of Pa-s) was calculated from the equation shown below.²⁹

$$\eta = \frac{\tau_R}{\dot{\gamma}_R} \tag{5}$$

A log–log plot of the viscosity η (in units of Pa-s) as a function of shear rate $\dot{\gamma}_R$ (in units of s⁻¹) is plotted in Figure 6 for the composites containing Ketjenblack EC-600 JD carbon black and in Figure 7 for the composites containing Thermocarb TC-300 synthetic graphite. All the data points collected are shown in these figures. It is clear that, over the range of shear

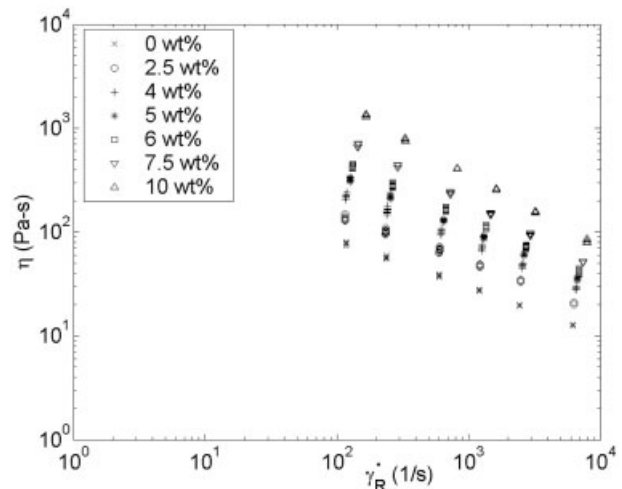


Figure 6 Rheology results for composites containing Ketjenblack EC-600 JD.

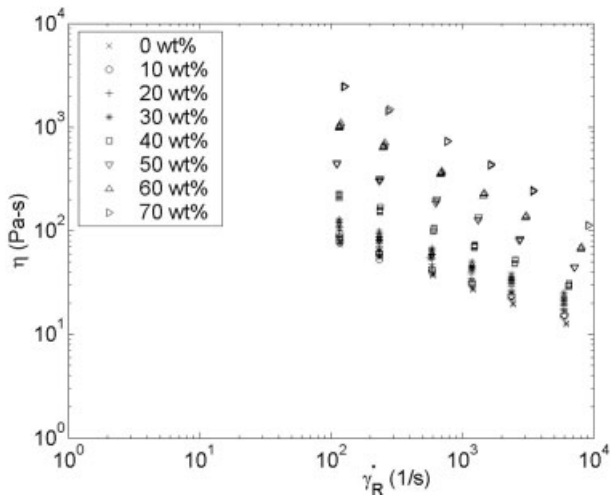


Figure 7 Rheology results for composites containing Thermocarb TC-300.

rates studied here, the fluid is shear-thinning. Furthermore, for the data obtained in this study, the η versus $\dot{\gamma}_R$ relationship is relatively linear, and thus the composites follow the power law model:

$$\eta = m\dot{\gamma}^{n-1} \quad (6)$$

where m is the consistency index (in units of $\text{Pa}\cdot\text{s}^n$) and n (dimensionless) is an exponent that shows the deviation from ideal (Newtonian) behavior.²⁹ Equation (6) above was best fit to each set of rheological data and the constants m and n are presented in Tables IV and V. The consistency index m increased as the filler loading was increased (from $690 \text{ Pa}\cdot\text{s}^{0.54}$ for pure Vectra A950RX to $\sim 10^4 \text{ Pa}\cdot\text{s}^{0.29}$ for highly filled composite materials), and the exponent parameter n typically decreased as the filler loading increased (from 0.54 for pure Vectra A950RX down to 0.29 for highly filled composite materials).

When solid filler is added to polymers, the classic effect is for the viscosity to rise at low shear rates.³⁸ The viscosity at high shear rates is usually affected to a lesser extent. This rise in low shear rate viscosity is due to the development of a yield stress in filled systems; once the yield stress is overcome, the steady viscosity is largely unaffected by the filler. The increase in viscosity we observed in the carbon-Vectra composites was at high shear rates, high enough to be unaffected by yield stress. The converging shape of our viscosity shear rate curves is consistent with other literature reports that filler effects become less pronounced at higher shear rates,³⁹ but the viscosity enhancement at high rates is larger for these composites than is typically seen. An increase in viscosity of half a decade is not uncommon over the volume fractions investigated,³⁹ while for our systems the viscosity enhancement was an order of magnitude, even at shear

rates of 10^4 s^{-1} . Lobe and White's⁴⁰ work on polystyrene filled with carbon black showed that, for their systems, no filler effect on viscosity was seen for volume fractions 10% and below, while an enhancement at all rates was seen for volume percents of 20 and 25%. For our carbon black (Ketjenblack)-Vectra composites, a pronounced viscosity enhancement is seen for all volume percents (1.9–12.1%).

The equation of Maron and Pierce for the variation of relative viscosity η_r with volume fraction of filler (ϕ) in a concentrated suspension has been found to fit many systems, even shear thinning systems, as long as the comparison is done at constant shear stress³⁹:

$$\eta_r = \frac{\eta(\phi)}{\eta(\phi=0)} = \frac{1}{\left(1 - \frac{\phi}{A}\right)^2} \quad (7)$$

The parameter A is related to a maximum allowable volume fraction of filler particles and a value of $A = 0.637$ would represent random close packing of spheres. Many systems follow this model with $A = 0.68$.³⁹ For our two systems, a plot of relative viscosity versus volume fraction at shear stress of 10^5 Pa yields the relationships shown in Figure 8. The Maron and Pierce model approximately describes the Thermocarb data with reasonable values of A . The Ketjenblack data, however, are qualitatively different, exhibiting an abrupt increase in viscosity at low volume fractions that is not related to the geometric constraints of the filler but is related, most probably, to the unique connective structures carbon black is known to form.¹²

During testing no significant die swell or entrance pressure losses were noted for either series of compos-

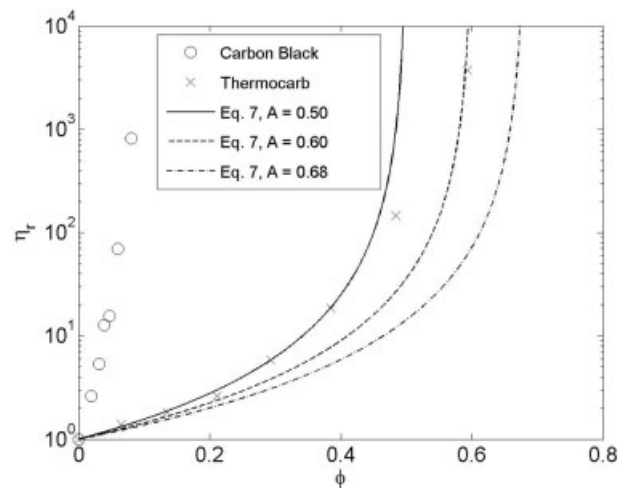


Figure 8 Relative viscosity versus filler volume fraction for Thermocarb and Ketjenblack composites at 300°C and shear stress of $100,000 \text{ Pa}$. Also shown are three model calculations.

ites. Vectra itself does not show these effects, and literature reports for other carbon-filled systems indicate that the addition of filler only reduces die swell and entrance pressure effects.³⁹

The surface texture of the extrudate from the capillary rheometer varied somewhat with filler volume fraction and with filler type. The bare Vectra extrudate has a characteristic glossy but mottled surface texture that reflects the crystalline structure of the solid. For the Thermocarb composites, the addition of filler gradually darkened the color of the extrudate, which remained glossy and had the Vectra surface texture. For the composites with the highest weight fractions of Thermocarb, however (50, 60, 70 wt %) the surface was matte. For the Ketjenblack composites, the changes in extrudate appearance were more complex. Even the lowest concentration composite (2.5 wt %) was deep black (compared to the dark gray Thermocarb 10 wt %), and all extrudates were glossy with the Vectra surface texture except the 5 wt % composite, which was matte. Also, the composites with the two highest concentrations of Ketjenblack, 7.5 and 10 wt %, exhibited kinks in the extrudate, reminiscent of mild melt fracture effects seen in polystyrenes at high rates of extrusion. The kinks in the Ketjenblack composites are long-periodicity distortions, on the order of 2–3 cm apart for the extrudates produced at high flow rate. The incidence of a matte surface texture in the 5 wt % Ketjenblack composites correlated with reaching the percolation threshold (4 vol %) in the resistivity measurements, but in the Thermocarb composites, the change to matte texture (at 50 wt %) occurred well after the percolation threshold (15 vol %).

The observed rheological results have implications for the manufacturing of bipolar plates. The results in Figure 6 show that at a $\dot{\gamma}_R$ of $\sim 1000 \text{ s}^{-1}$, the viscosity η increases from 28 Pa-s for the neat Vectra to 260 Pa-s for the composites containing 10 wt % (8 vol %) Ketjenblack EC-600 JD. This order of magnitude increase in viscosity will make composites containing 10 wt % Ketjenblack more difficult to injection mold into bipolar plates. At a $\dot{\gamma}_R$ of $\sim 1000 \text{ s}^{-1}$, the composites containing 5 wt % Ketjenblack EC -600 JD (3.9 vol %), which is near the electrical percolation threshold of 4 vol %), had a viscosity η of 90 Pa-s, which is three times that of the neat Vectra. It appears that the highly branched carbon black structure causes a threefold increase in viscosity near the percolation threshold.

As noted earlier, the increase in viscosity for the Thermocarb composites is more gradual than the viscosity increase in the carbon black composites. Figure 7 shows that the viscosity is essentially the same for the neat (pure) Vectra and the composites containing 10 wt % (6.5 vol %) and 20 wt % (13.5 vol %) Thermocarb TC-300. Then, above the electrical percolation threshold of 15 vol %, the viscosity increases (note the separate distinct data points in Fig. 7) for the compos-

ites containing 30 wt % (21.1 vol %) Thermocarb. This effect appears to be related to the space-filling effect described by the Maron and Pierce equation. At a $\dot{\gamma}_R$ of $\sim 1000 \text{ s}^{-1}$, the viscosity η increases from 28 Pa-s for the neat Vectra to 430 Pa-s for the composites containing 70 wt % (59.3 vol %) Thermocarb TC-300. Again, this viscosity increase of ~ 15 times will make these highly filled composites more difficult to injection mold into bipolar plates. Based on the ER and viscosity results obtained in this study, the authors speculate that it will be possible to injection mold a material whose ER $< 1 \text{ ohm-cm}$ by using a combination of different carbon fillers, a mold temperature of $\sim 150^\circ\text{C}$, and a specially designed bipolar plate mold. This will be the topic of future papers.

CONCLUSIONS

The goal of this project was to determine the electrical resistivity and rheology of composites containing varying amounts of a single type of filler, either Ketjenblack EC-600 JD or Thermocarb TC-300 synthetic graphite, in Vectra A950RX LCP. The electrical percolation threshold was 4 vol % for composites containing Ketjenblack and 15 vol % for composites containing Thermocarb. Over the range of apparent shear rates from 100 to 5000 s^{-1} , all these materials followed a shear-thinning power law model. Adding the carbon fillers caused the neat Vectra consistency index m to increase from $690 \text{ Pa-s}^{0.54}$ to $\sim 10^4 \text{ Pa-s}^{0.29}$ for the highly filled composites. The enhancement of high shear rate viscosity due to the presence of the fillers was large, reaching nearly a decade even at shear rates of 10^4 s^{-1} . Viscosity enhancement in the Thermocarb materials appears to be related to a space-filling effect, while for the Ketjenblack composites a more specific structure development is likely the cause.

The authors gratefully thank the American Leistriz technical staff for recommending an extruder screw design. The authors thank Asbury Carbons and Akzo Nobel for providing carbon fillers. The authors thank Albert V. Tamashausky of Asbury Carbons for providing technical advice. The authors also thank the following undergraduate students for their assistance on this project: Nils Klinkenberg, James Simoneau, and Kelly Griffioen.

References

1. Taipalus, R.; Harmia, T.; Zhang, M. Q.; Friedrich, K. *Compos Sci Technol* 2001, 61, 801.
2. Agari, Y.; Uno, T. *J Appl Polym Sci* 1985, 30, 2225.
3. Bigg, D. M. *Polym Eng Sci* 1977, 17, 842.
4. Bigg, D. M. *Adv Polym Technol* 1984, 4, 255.
5. Narkis, M.; Lidor, G.; Vaxman, A.; Zuri, L. *J Electrostat* 1999, 47, 201.
6. Nagata, K.; Iwabuki, H.; Nigo, H. *Compos Interfaces* 1999, 6, 483.

7. Demain, A. Thermal Conductivity of Polymer-Chopped Carbon Fibre Composites, Ph.D. Dissertation, Universite Catholique de Louvain, Louvain-la-Neuve, Belgium, 1994.
8. King, J. A.; Tucker, K. W.; Meyers, J. D.; Weber, E. H.; Clingerman, M. L.; Ambrosius, K. R. *Polym Compos* 2001, 22, 142.
9. Murthy, M. V. Proceedings of the Society of Plastics Engineers Annual Technical Conference, 1994, 1396.
10. Simon, R. M. *Polym News* 1985, 11, 102.
11. Mapleston, P. *Mod Plast* 1992, 69, 80.
12. Donnet, J.-B.; Bansal, R. C.; Wang, M.-J. *Carbon Black*, 2nd ed.; Marcel Dekker: New York, 1993.
13. Huang, J.-C. *Adv Polym Technol* 2002, 21, 299.
14. Bigg, D. M. *Polym Compos* 1987, 8, 1.
15. Wilson, M. S.; Busick, D. N. U.S. Pat. 6,248,467 (2001).
16. Loutfy, R. O.; Hecht, M. U.S. Pat. 6,511,766 (2003).
17. Braun, J. C.; Zabriskie, J. E.; Neutzler, J. K., Jr.; Fuchs, M.; Gustafson, R. C. U. S. Pat. 6,180,275 (2001).
18. Mehta V.; Cooper, J. S. *J Power Sources* 2003, 114, 32.
19. Ticona Vectra Liquid Crystal Polymer (LCP) Product Information, Ticona, Summit, NJ, 2000.
20. Chiou, J. S.; Paul, D. R. *J Polym Sci Part B: Polym Phys* 1987, 25, 1699.
21. Akzo Nobel Electrically Conductive Ketjenblack Product Literature, Chicago, IL, 1999.
22. Asbury Carbons Product Information, Asbury, NJ, 2004.
23. Conoco Carbons Products Literature, Conoco, Houston, TX, 1999.
24. Clingerman, M. L.; King, J. A.; Schulz, K. H.; Meyers, J. D. *J Appl Polym Sci* 2002, 83, 1341.
25. Clingerman, M. L.; Weber, E. H.; King, J. A.; Schulz, K. H. *J Appl Polym Sci* 2003, 88, 2280.
26. *Plastics—Standard Atmospheres for Conditioning and Testing*, ISO 291:1997; ISO: Switzerland, 1998.
27. *Standard Test Methods for DC Resistance or Conductance of Insulating Materials*, ASTM D257-91; ASTM: Philadelphia, 1998.
28. Heiser, J. A.; King, J. A.; Konell, J. P.; Sutter, L. L. *Adv Polym Technol* 2004, 23, 135.
29. Morrison, F. A. *Understanding Rheology*; Oxford University Press: New York, 2001.
30. *Standard Test Methods for Determination of Properties of Polymeric Materials by Means of a Capillary Rheometer*, ASTM D3835-02; ASTM: Philadelphia, 2002.
31. Bagley, E. B. *J Appl Phys* 1957, 28, 624.
32. King, J. A.; Miller, M. G.; Barton, R. L.; Keith, J. M.; Hauser, R. A.; Peterson, K. R.; Sutter, L. L. *J Appl Polym Sci*, to appear.
33. Heiser, J. A.; King, J. A. *Polym Compos* 2004, 25, 186.
34. Weber, M.; Kamal, M. R. *Polym Compos* 1997, 18, 711.
35. Onogi, S.; Asada, T. In *Rheology*; Astarita, G., Marrucci, G., Nicolais, L., Eds.; Plenum: New York, 1980.
36. Wissbrun, K. F. *J Rheol* 1981, 25, 619.
37. Gotsis, A. D.; Baird, D. G. *J Rheol* 1985, 29, 539.
38. Chapman, F. M.; Lee, T. S. *SPE J* 1970, 26, 37.
39. Dealy, J. M.; Wissbrun, K. F. *Melt Rheology and its Role in Plastics Processing*; Van Nostrand Reinhold: New York, 1990.
40. Lobe, V. M.; White, J. L. *Polym Eng Sci* 1979, 19, 617.